ISSN: 2753-4154 (Online)

Type of the Paper (Article)

Using low-cost UAVs in post-mining exploration - a case study

Jakub Markiewicz [1,*], Sławomir Łapiński[2], Magdalena Pilarska-Mazurek[1], Dorota Zawieska[1] and Volodymyr Levytskyi[3]

[1] Department of Photogrammetry, Remote Sensing and Spatial Information Systems, Faculty of Geodesy and Cartography, Warsaw University of Technology, sqr. Politechniki 1, Warsaw 00-661, Poland; jakub.markiewicz@pw.edu.pl (J.M.), magdalena.pilarska@pw.edu.pl (M.P.), dorota.zawieska@pw.edu.pl (D.Z.)

[2] Department of Engineering Geodesy and Measuring Systems, Faculty of Geodesy and Cartography, Warsaw University of Technology, Plac Politechniki 1, Warsaw 00-661, Poland; slawomir.lapinski@pw.edu.pl (S. Ł.),

[3] Department of Mine Surveying, Zhytomyr State Technological University, Zhytomyr, Ukraine; v.levytskyi@ztu.edu.ua (V.L.)

***** Correspondence: jakub.markiewicz@pw.edu.pl; Tel.: +48-22-234-5764

Received: 02/06/2022; Accepted: 28/06/2022; Published: 31/08/2022

Abstract: The use of low-cost, unmanned aerial vehicles (UAVs) has been growing in many sectors. Due to the sufficient accuracy of the products acquired from UAVs, this technology has also been applied in geodesy and remote sensing. It results from many factors: the low prices of UAVs and the availability of different sensors and software applications, which allows for simple data processing. Due to the required high accuracy, the inventory of a mine is usually performed with the use of conventional surveying techniques, such as tacheometry. This paper discusses the possibilities of applying low-cost UAVs to inventory open-cut mining. Using Phantom 3 Professional equipped with a factory-made camera, RGB photographs were acquired, which were then processed using three commercial software applications: Pix4D, 3D Survey and Agisoft Metashape. Different algorithms for image orientation (Structure-from-Motion, SfM) and dense point generation (Multi-View Stereo, MVS) were implemented for each of those applications, which influenced the accuracy of the final products. The results of the experiments proved that the highest accuracy in terms of photograph processing was achieved using the Pix4D software. The mean difference between the DTM (Digital Terrain Model) generated from surveys, and the DTM generated from photographs using Pix4D was equal to 0.106 m. This paper compared the DTMs and the DSMs (Digital Surface Models) generated by the selected software applications. The models generated with the use of Pix4D were assumed as a reference. According to the analysis of the DTMs and the DSMs, the smallest differences were obtained for the models generated by Pix4D and Agisoft Metashape. They equalled 0.080 m for the DTM and 0.246 m for the DSM. The differences between the DSMs generated by Pix4D and 3D Survey were two times bigger; the differences between the DTMs generated by those software applications were six times bigger. The differences between the models may result from the presence of vegetation and escarpments at the edges of the test site and different algorithms for generating dense point clouds applied in particular applications.

Keywords: low-cost UAV/UAS; structure-from-motion; SfM, multi-view-stereo, MVS, post-mining exploration, quality assessment, comparison Pix4D, Agisoft Metashape, 3D Survey.

1. Introduction

One of the basic tasks of surveying services for a mining plant is to perform surveys related to the construction, development and operation of such a plant, including the determination of caprock and excavated minerals (§ 155 of the Decree of the Minister of Economy of April 8, 2013)[1]. To ensure the security of mining operations and to organise those operations efficiently, an accurate and currently updated map of a mining site is required, covering both the site of the works and the excavation heaps. It is also necessary to currently/periodically perform inventorying measurements, including monitoring the progress of the deposit exploitation, monitoring the removal of caprock, the determination of the area and volume of the excavated minerals and dumps, as well as the determination of the size of the re-cultivated sites. Besides, works aiming at the assessment of the stability of the escarpments and slopes of the excavation, as well as dumps, are performed together with the examination of the movements of the rock masses in the direct and indirect neighbourhood of the open-mining and movements of bing masses, as well as the determination of the safe height of dumps [2,3].

The development of mining technology and the exploitation methods of open mines makes it difficult - and sometimes impossible - to develop accurate mining maps using conventional surveying methods, namely tacheometry and GNSS (RTK). They are currently substituted by modern and faster methods, such as laser scanning and digital, aerial or terrestrial photogrammetry, LiDAR, InSAR and unmanned aerial vehicles (UAV). This makes it possible to improve the security level within a mine and the effectiveness and ergonomics of the performed surveys due to the limitation of the number of field workers and to focus on laboratory works in inventorying measurements [2].

This paper aims to analyse the algorithms' results and effectiveness in processing low-cost UAV data acquired for an excavation area and the post-mining site, implemented in the selected software applications - Pix4D, Agisoft and 3D Survey. In this paper, the extended Digital Surface Model (DSM) accuracy analyses based not only on ground control points (GCPs) (commonly used) but also on dense GNSS RTK measurements of the terrain surface were performed.

1.1 Measurement methods

In small open mines, surveys are mostly performed using total stations. The implementation of surveys includes the determination of characteristic features from the total station [3]. This method allows for achieving high accuracy of surveys and recording characteristic terrain features in areas which are hardly accessible for other surveying techniques. The basic disadvantage of total station measurements is the time of the operations, influenced by the terrain relief specification and increasing in line with the growing number of terrain features.

Another method typically used in open pit mining monitoring is the GNSS/RTK method, which makes it possible to achieve a measurement accuracy of +-2 cm in the horizontal components and +-5 cm for elevations within a short observation time above a point. As the sole technology among relative satellite methods, the RTK meets the criteria required for the inventory of mine dumps and dumping grounds [4]. The basic advantages of this method, i.e. the possibility to perform measurements in any weather conditions, at any time of the day and the possibility to simultaneously determine three coordinates of a measured point in an assumed reference system, resulted in its regular use for the needs of inventorying measurements and monitoring of open mines [5].

DOI:10.55627/smla.001.01.0009

The terrestrial laser scanning (TLS) technology has recently become one of the most modern survey techniques [5,6]. Data from scanning may also be applied for the measurements of the deformations of the terrain surface and for the monitoring of landslides, which are created inside the excavations and dumping sites [7], as well as for the inventory and monitoring of the installations and facilities of a mining plant [8]. It is recommended to apply this method in smaller open mines due to the reduced size of the areas, the geometry of the excavations and the advantageous conditions of the measurements [2].

In the context of open mines, photogrammetry makes it possible to obtain data and reconstruct models and, therefore, to record the current conditions of the excavations; this is important for the calculations of the excavated minerals and removed caprock [9]. The possibility of achieving the high accuracy of photogrammetric processing highly depends on different factors, which will be widely described in the next section [2, 10].

Nowadays, unmanned aerial vehicles (UAVs) [11], which are commonly known as drones and were initially applied for military purposes, are widely used for different commercial purposes such as the monitoring of line objects [12] and precise agriculture [13], cultural heritage etc.

UAVs have also been applied in geological sciences and mining [14,15,16,17,18,19], where they have become the alternative to conventional field surveys. The additional advantage of using UAVs is represented by the remote data acquisition, which results in increased security of measurements [17]. The basic products of those measurements include a 3D model of a mine [16, 19], as well as orthomosaics used to monitor the surface of post-mining lakes [20]. Additionally, 3D models of mines are used for the calculation of earth masses [17]. In many cases, the photographs acquired by UAVs are used to detect dodges in geological structures [21].

UAVs carry sensors (laser scanners, RGB, NIR, thermal and hyperspectral cameras), which generate many products [14]. They include orthophotomaps, digital terrain models, dense point clouds, and 3D models of objects [14,18].

1.2 The potential and limitation of UAVs in mining and post-mining exploration

According to the literature, there are already some articles published in which the UAV DTM was compared to the GNSS measurements [22]. However, the authors indicate the limitations and difficulties resulting from using low-cost UAV solutions. The rolling shutter effect can impact the accuracy of the UAV products. Therefore, rolling shutter models are implemented. In Pix4D, two rolling shutter models are included, namely the global shutter and the linear rolling shutter [23]. In Agisoft Metashape, the skew parameter determines the image self-calibration algorithm. Another possibility of reducing the impact of the rolling shutter is decreasing the UAV flight velocity. In [24], reference is made to the difficulties related to time synchronisation, limited image exposure control, and the overlap of images. The GoPro camera, which was used in the experiment, has a short focal length, which results in barrel lens distortion. The authors [25] emphasise the sufficient influence of image distortion on orthophoto accuracy. Image distortion can influence the accuracy of dense point cloud generation. The UAV images were obtained on the rugged terrain, and the distortion correctness improved the results [26]. In [27], the authors notice that mines are usually in mountainous areas. Therefore, it is necessary to properly plan and conduct the UAV campaign for the photogrammetric mapping of open-pit mines and their surroundings. It could be difficult to avoid the registration problems on the big slopes. Therefore, TLS measurements are integrated with the UAV mission. Furthermore, open-pit mines may be characterised by a poor texture. UAV solutions, which can be explored in the mining inventory, are usually equipped with low-cost cameras. Thus, better cameras would also increase the measurement accuracy [28]. Moreover, the cameras mounted on low-cost UAV solutions are characterised by a small sensor size, which may render the image orientation

DOI:10.55627/smla.001.01.0009

and 3D modelling process more difficult [16]. Images may also be characterised by low contrast. Furthermore, areas with significant height differences that might occur in shadows may be registered. In [29], an image pre-processing was performed, and contrast enhancement and shadow removal were implemented. However, the accuracy improvement was not observed. The vertical accuracy increased from 1.72 cm to 1.62 cm. Additionally, in the time of UAV technology development, an alternative solution to the UAV images can be the usage of UAV laser scanning in mining. In [30], the authors suggest using UAV Lidar to calculate volume in one of the largest open-pit mines in Poland.

1.3 Software and algorithms used

Modern software packages dedicated to processing terrestrial and aerial images utilise algorithms based on a combination of methods commonly applied in ComputerVision (CV) and algorithms applied in conventional photogrammetric works [31,36]. The algorithms applied for those purposes allow for the complete automation of orientation and data processing.

Algorithms of automatic matching and processing of photographs (SfM - Structure-from-Motion and MVS - Multi-View Stereo) are commonly applied to generate different photogrammetric products used in the inventory of mines based on digital images. Both open-source and commercial (Pix4D, Agisoft, 3D Survey) software packages are available on the market. Those packages apply different algorithms, which are often not described by manufacturers. However, it is generally known based on the SfM (used in the orientation process) and MVS (used for the dense point cloud generation) approach [18,32,33,34,35]. The SfM pipeline is based on four steps: (1) detection of the key-points based on BLOB algorithms [32,36,37], (2) description of detected key-points, (3) preliminary image point matching, (4) reconstruction of the image acquisition geometry and referencing of the intrinsic coordinate system to available reference points (either GPS or known camera locations) using an iterative bundle adjustment.

Another issue, which should be considered when the images from UAV with mounted low-cost cameras are processed in the SfM process, is the rolling shutter effect [38]. This effect is considered only by some software packages available on the market. The advantage of the Pix4D package over Agisoft Metashape is the possibility of reducing the rolling shutter effect. This effect often occurs in cameras that record images line by line during the fast motion of the camera. Changes in objects' positions during image acquisition may influence the possibility of matching photographs and, therefore, the accuracy of the photographs' orientation and the resulting products, such as point clouds.

The MVS approach is used for a dense point matching of the sparse cloud from the image network geometry. Based on a different strategy regarding the generation of a dense point cloud, three different methods are distinguished: i.e. depth map fusion (which is implemented in Agisoft Metashape) [39,40], region growing [34,41] and Semi-Global Matching (SGM) [42,43].

In the final step consisting of the meshing of the dense point cloud, a digital surface model (DSM) can be obtained from this or the previous step, as well as calculating the textures from the images to compute the rectified orthomosaic.

3. Study area and methodology

DOI:10.55627/smla.001.01.0009

The experiment was performed within the quartz sand mine in Trzciniec, neighbouring Bydgoszcz, Poland. The mineral deposits used to produce limestone-and-sandy bricks are located there. Its area equals approximately 62 hectares, but the experiment covered an area of approximately 10 hectares, Fig. 1a). The mine has been operating since 1970, without interruptions. More than 4.2 million tonnes of sand were excavated to produce silicates. The area is the post-mining, partially re-cultivated area.

Performed works included direct field measurements using the GNSS RTK technique (HiperPro Topcon receiver, FC-200 controller with software), total station (Leica TS09) and photogrammetric flight with the use of the UAV - Quadrocopter Phantom 3 Professional.

3.1. Photogrammetric flight with the use of UAS/UAV

After analysing the shape of the excavation, the flight consisting of three blocks of photographs was planned; they had a common part in the central part of the area (Fig. 1b).

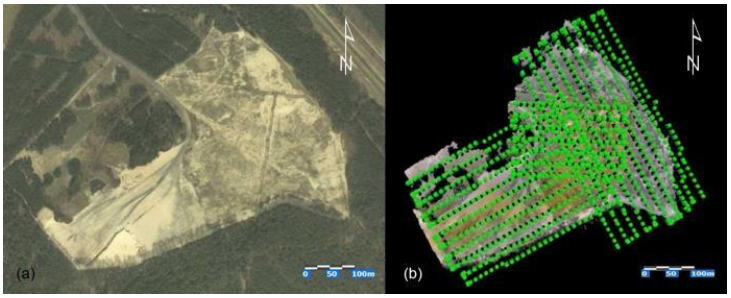

Figure 1. a) The excavation, b) Photogrammetric flights above the test site - an excavation of the Trzciniec mine, Poland

For image orientation (bundle adjustment process), 17 ground control points were planned; they were signalled using marks with the pattern of a black-and-white chessboard (Fig. 2.) of dimensions 0.5 x 0.5 m; they were used to adjust the photographs acquired from UAVs. The coordinates of the temporarily stabilised points were measured using the GNSS RTK technique. Control (11) and check (6) points were planned in the ground control to maintain the inspection of the accuracy of the adjustment process. It was decided to maintain redundant control points to perform different types of adjustments and ensure sufficient data for the experiments. Their distribution within the analysed area is presented in Fig.2.

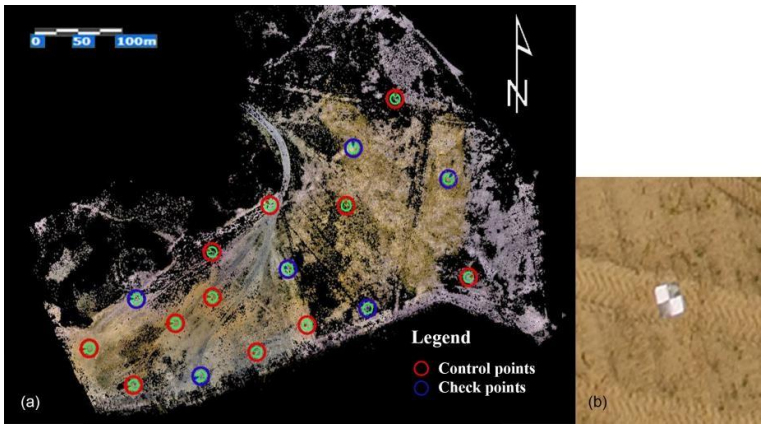

Figure 2. Distribution of the points of the ground control (a) within the mine and the enlarged pattern of a control point of the size 0.5 x 0.5 m (b)

DOI:10.55627/smla.001.01.0009

During flights (with an average velocity of 7 m/s), which lasted 30 minutes, 912 photographs were acquired. The flight altitude equalled approx. 35 m AGL, which resulted in the mean GSD value at the level of 1.6 cm. 70% of the side overlap and 60% of the side overlap of the photographs were maintained. Due to the proximity of the Bydgoszcz Szwederowo International Airport, the time and conditions of the flight had to be adapted to binding procedures. One of them was related to the limitations of the flight altitude, which made it impossible to perform wider tests related to the investigations of the influence of flight altitude on the efficiency and accuracy of the processing of a mining plant.

3.2. Field GNSS and total station measurements

For the independent accuracy analysis, the terrain relief was measured using the GNSS (Global Navigation Satellite System) in the RTK (Real-Time Kinematic) mode. The RTK measurement was performed using one GNSS receiver with corrections to the position from the TPI-NET system. The TPI-NET system is a network of GNSS reference stations evenly distributed within Poland, which transmit corrections to the receiver's position in real-time. The measurement in the RTK mode allows for a fast determination of the X, Y, and H positions of the measured point, with horizontal accuracy equal to 2 cm and vertical accuracy of 3 cm. Close to the forest, some points were measured using a conventional electronic total station, due to the influence of trees, which results in problems concerning the reception of GNSS signals (it was not able to achieve the "fixed" solution). Figure 3 shows the distribution of 1542 GNSS/RTK and total station measured terrain points used for checking the quality of dense points clouds.

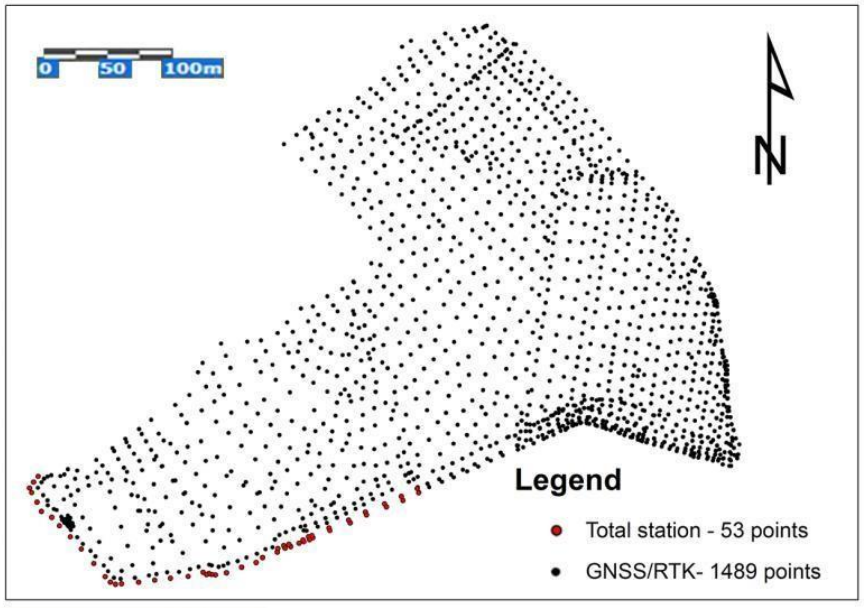

Figure 3. Distribution of the terrain points used for checking the quality of dense points clouds

To correctly reflect the terrain relief on the map, the spot heights were measured in the following places:

- at peaks, saddles and in the lowest area of the terrain,
- on the upper and bottom edges of slopes,
- for escarpments, excavations and other man-made forms, the spot heights were distributed on the edges of the planes and in characteristic points, which reflected the spatial arrangement of the area.

DOI:10.55627/smla.001.01.0009

The escarpments were not generalised, regardless of their dimensions. In places of breakdowns of escarpments, the spot heights were situated on the top and bottom of an escarpment. In the areas of uniform terrain relief, the characteristic spot heights were measured within a distance of 20-30 meters.

4. Results

The important element of data processing acquired from different sources is selecting a common and unified spatial reference system. In the case of plain coordinates, the PUWG 2000/6 system (The State Geodetic Coordinate System) was assumed based on 3-degree belts in the modified Gauss-Kruger projection of the scale factor m0=0.999923. Normal heights referenced to the Kronsztadt'89 system were assumed as the system of elevations. It is the spatial reference system obligatory in Poland.
The data acquired from the GNSS observations (from the receiver used for the RTK measurements and from the receiver on the UAV) and total station are referenced to the global spatial reference systems, to the WGS 84 ellipsoid; each measured point has its B, L, H coordinates, where B - geographical latitude, L - geographical longitude, H - ellipsoidal elevation. Those values are automatically re-calculated by the software to X, and Y coordinates of the system 2000, based on commonly accessible formulae. Ellipsoidal elevations are automatically re-calculated onto normal heights. Within the performed experiments, the products were generated: the point cloud, the point cloud filtered to the ground, the DTM (Digital Terrain Model) and the DSM (Digital Surface Model).

4.1 UAV image orientation

The parameters and reports generated by each software are slightly different. However, the main principle of processing photos is similar, and it is possible to compare the results and corresponding settings. The main parameters and numbers are presented in Tab. 1. After the first step (called in software 'Bundle adjustment' or 'Point cloud generation'), some significant differences in the number of tie points can be observed. Agisoft Metashape has the best-performing algorithm on this matter. In each software, the camera's alignment was performed using full resolution (original images), not using one of the image pyramids. The image pair selection method is described, except for 3D Survey, where such an option is not available. The table also presents the dense cloud generating parameters. It clearly shows that Agisoft and Pix4D outperformed 3D Survey in cloud density. Although Pix4D has fewer tie points in the sparse point cloud, it performed similarly to Agisoft with a densified points number, which needs to be mentioned.

Table 1. Processing software main parameters

Agisoft Metashape		**Pix4D**		**3D Survey**	
Point Cloud		**Bundle Block Adjustment**		**Bundle Adjustment**	
Points	3,28 mln	3D tie points	1,93 mln	3D tie points	0,54 mln
Alignment		**Initial Processing**		**Alignment**	
Accuracy	High	Image scale	Full (original)	Image scale	Full (original)
Pair preselection	Reference	Image pairs	Aerial Grid or Corridor	Image pairs	no data
Dense Cloud		**Point Cloud**		**Dense Cloud**	
Point Quality	High	Point density	High	Point density	Extreme
No. of points	224 mln	No. of points	220 mln	No. of points	14 mln

DOI:10.55627/smla.001.01.0009

In order to compare the products obtained by means of selected software packages, different aspects related to the processing of photographs and the generation of products were analysed.

- The time of operation of the SfM and MVS modules for particular packages (Tab. 2),
- The number of matched photographs (Tab. 3),
- Analysis of the number of tie points and the accuracy of the DSM resulting from tie points (the accuracy of the SfM process) (Tab. 4).

Table 1 presents the results concerning the time of detection, matching of tie points and bundle adjustment using the Structure-from-Motion algorithms implemented in the AgiSoft, 3D Survey and Pix4D software packages. Moreover, the time of the dense point cloud generation was also tested.

Table 2. Operation times of the SfM and MVS modules for particular software applications

Software	Time of orientation of photographs [h]	Time of generation of a dense point cloud [h]
Pix4D	2.0	5.0
3D Survey	2.0	12.0
Agisoft Metashape	4.5	8.5

It turns out from the results of the analysis presented in Tab.2 that the shortest time of detection, matching characteristic points, and bundle adjustment was achieved using the Pix4D and the 3D Survey packages. Comparing the time of operation of the SfM algorithm implemented in Agisoft Metashape, it may be noted that it is two times longer than for the two other packages.

When considering the time of generation of dense point clouds, it may be concluded that the shortest times were achieved for Pix4D, Agisoft Metashape and 3D Survey, respectively. The time of processing using the 3D Survey package was almost two times longer.

Table 3. The number of matched photographs

Software	The number of correctly matched photographs	Percentage of the number of correctly matched photographs [%]
Pix4D	798	87.5
3D Survey	703	77.1
Agisoft Metashape	772	84.6

The factor which is decided the effectiveness of the SfM algorithms is the number (and the percentage) of correctly matched photographs (Tab.3). Comparing the results for particular packages, it may be noticed that the highest number of photographs were matched using Pix4D, the second result was obtained for Agisoft, and the least number of photographs were matched using 3D Survey. That was the reason for checking the distribution of photographs, which were not matched correctly (Fig. 4).

DOI:10.55627/smla.001.01.0009

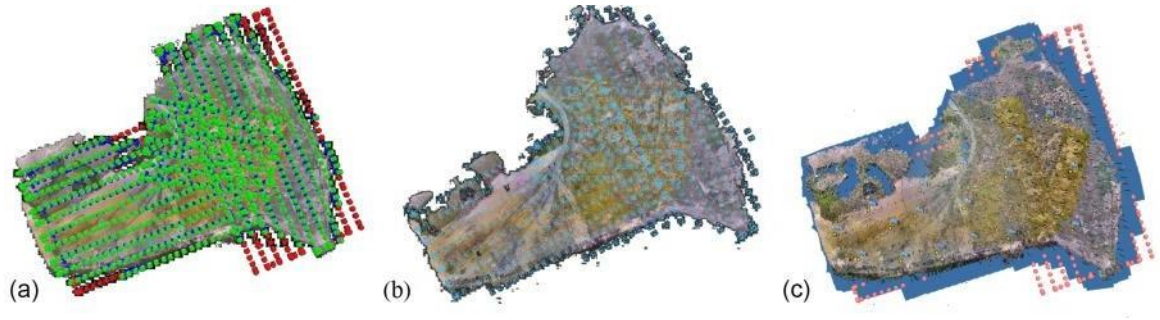

Figure 4. Distribution of the projection centres of the photographs: a) Pix4D, correctly matched photographs marked in green, red marks photographs, which have not been oriented, b) 3D Survey, blue rectangles present correctly matched photographs, c) Agisoft Metashape, blue rectangles mark correctly matched photographs, pink dots - incorrectly oriented photographs

All tested software packages presented some difficulties with the explicit identification of tie points at the edges of the processed blocks of photographs (in the re-cultivated part of the area, covered by medium and high vegetation, where small differences in the terrain elevations occur), in the centre of the northern part (the area covered by high vegetation) and at the edges in the SW part (close to the escarpments). Moreover, the algorithms implemented in the 3D Survey package did not orientate all photographs in the triple overlap belt and the NW part of the block.

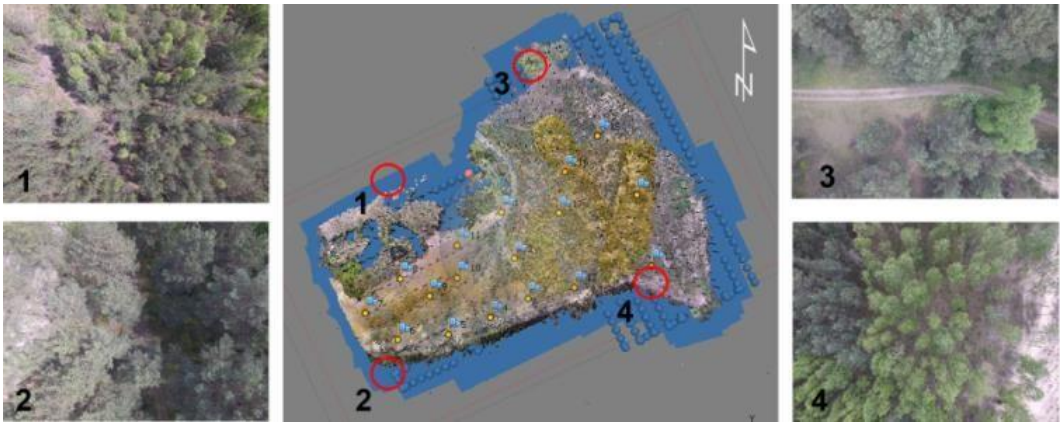

Figure 5. Distribution of the projection centres of the photographs with examples of photographs where the tie points have not been discovered and matched by the SfM algorithms

Difficulties concerning detecting and matching the tie points (using SfM algorithms) were mainly related to the presence of low and high vegetation within fragments of the re-cultivated part of the mine (Fig. 5).

Table 4. Analysis of the number of tie points and the accuracy of the DSM generated based on tie points (the accuracy of the SfM process)

Software	The number of tie points	RMS reprojection error [px]	Max reprojection error [px]
Pix4D	5466641	0.3	no data
3D Survey	542324	1.6	7.3
Agisoft Metashape	3278115	1.4	131.3

DOI:10.55627/smla.001.01.0009

Other factors, which are decided for the correctness of the orientation process and mutual matching of photographs acquired from the low-cost UAV, are the RMSE and max reprojection error values [44].

The homography that relates every point of the pattern object depicted in a real world frame with the corresponding point of the pattern image is expressed by an invertible 3x3 matrix with the use of homogeneous coordinates:

$$\begin{matrix} x_{frame} \\ [y_{frame}] \\ 1 \end{matrix} = \begin{matrix} h_{11} & h_{12} & h_{13} \\ [h_{21} & h_{22} & h_{23}] \\ h_{31} & h_{32} & h_{33} \end{matrix} \begin{matrix} x_{pattern} \\ [y_{pattere}] \\ 1 \end{matrix} \quad (1)$$

where: x_{frame}, y_{frame} - are the pixel coordinates of a point in a frame,

$x_{pattern}, y_{pattern}$ - are the pixel coordinates of the same point in the pattern image,

h_{ij} - are the elements of the homography matrix.

As a result of the knowledge of the relative orientation parameters of the photographs, the RMSE reprojection error value is calculated, which determines the correctness of the matching of photographs:

$$\text{RMSE} = \sqrt{\frac{\sum(x_{frame} - x'_{frame})^2}{m-9}}, \quad (2)$$

where: x_{frame} - are the coordinates of a point in a frame,

x'_{frame} - are the pixel coordinates of the same point in the pattern image transformed to the point in a frame coordinate system based on the homography matrix,

m - number of homogenous points.

The high reprojection error value proves the low accuracy of tie point matching, which may result from the insufficient key-point description and matching. Table 3 presents the number of tie points with the RMSE accuracy and the maximum and the minimum reprojection error values. It turns out from the analysis of Table 3 that the majority of tie points were determined using the Pix4D package, and the lowest number thereof was determined using the 3D Survey package. Besides, the highest accuracy of tie points was achieved in the Pix4D package, and it was several times higher than in the case of other packages. The high value of the maximum error for the Agisoft package seems disturbing; it may point to the incorrect matching of a tie point. In summary, it may be stated that the similar, low RMSE reprojection error value for all packages proves the correctness of processing.

One of the most important stages, which influences the completeness and correctness of the resulting photogrammetric products, is the process of exterior photograph orientation. It consists of the determination of three linear and three angular parameters, which describe the position of a photograph in the space. This process is performed based on signalled control points with the use of Equation 3:

DOI:10.55627/smla.001.01.0009

$$\lambda \begin{bmatrix} x_{frame} \\ y_{frame} \\ 1 \end{bmatrix} = K[R|t] \begin{bmatrix} X \\ Y \\ Z \\ 1 \end{bmatrix}$$

$$\lambda \begin{bmatrix} x_{frame} \\ y_{frame} \\ 1 \end{bmatrix} = \begin{bmatrix} c_x & 0 & x_0 \\ 0 & c_y & y_0 \\ 0 & 0 & 1 \end{bmatrix} \begin{bmatrix} r_{11} & r_{12} & r_{13} & t_1 \\ r_{21} & r_{22} & r_{23} & t_2 \\ r_{31} & r_{32} & r_{33} & t_3 \end{bmatrix} \begin{bmatrix} X \\ Y \\ Z \\ 1 \end{bmatrix} \quad (3)$$

where: X, Y, Z are the object coordinates of a point x_{frame},y_{frame} in the frame,
K is the matrix with the camera intrinsic parameters,
$[R|t]$is the joint rotation-translation matrix with the camera extrinsic parameters,
λ is a scale factor.

The accuracy related to determining the coordinates of the control points is usually considered in Equation 3. It is possible to perform this using Agisoft and Pix4D; the 3D Survey package did not offer this special feature. To perform an independent control, deviations are analysed on check points based on the orientation elements determined using Equation 3. The factor which decides the correctness of the performed process in the RMSE error value (4):

$$\mathrm{RMSE} = \sqrt{\frac{\sum(X-X')^2}{m-n}}, \quad (4)$$

where: X - vector of coordinates of points in the external coordinate system,
X' - vector of coordinates of points calculated based on the determined elements of exterior orientation,
m - number of observations
n - number of control points

Table 5 presents the accuracy analysis of the orientation process on ground control (11) and check (6) points.

Table 5. Accuracy analysis of the data orientation process on the ground control (11) and check (6) points

Software	Ground control points			Check points		
	RMSE			RMSE		
	X [m]	Y [m]	Z [m]	X [m]	Y [m]	Z [m]
Pix4D	0.006	0.005	0.019	0.015	0.014	0.051
3D Survey	0.013	0.017	0.009	0.140	0.186	0.336
Agisoft Metashape	0.099	0.113	0.110	0.071	0.160	0.289

The highest accuracy of the orientation of the control type points was obtained, respectively, using the algorithms implemented in the Pix4D, 3D Survey and Agisoft Metashape packages. It should be noted that the accuracy of the matching photographs in the terrain system performed using Agisoft Metashape was lower by one order compared to the remaining packages. For the Agisoft and 3D Survey results, the RMSE error values are similar for all components. For the Pix4D package, the error values of the Z component are 3-4 times higher than for the XY components. It turns out from the analysis of the RMSE error values on the check type indicates that all the obtained values are higher than for the tie points. Comparing the obtained results for particular components, it may be concluded that the Z component value is considerably higher than in the case of the XY components.

DOI:10.55627/smla.001.01.0009

This may prove the presence of the systematic error resulting from the task concerning the determination of deviations between the geoid and the ellipsoid. The difference in values obtained using the Pix4D and 3D Survey packages from the values obtained with Agisoft Metashape (almost four times) results from the fact that the first two algorithms have embedded functions for determining approximate deviation values between the geoid and the ellipsoid. Despite this, obtained values of the accuracy of the orientation meet the accuracy requirements of the determination of the point positions required for the measurements of post-mining objects and the terrain relief.

4.2 Dense point cloud and DTM analysis

During the next stage, the quality of point clouds was analysed. For this purpose, the ArcGIS application was applied to generate different cartographic presentations; the original software application in the Matlab environment was also applied to perform a statistical analysis and generate histograms of the tested values.

Firstly, to assess the quality and correctness of the generated point cloud, the number of points per 1 sq.m. in the raw point cloud, generated with the assumption of the highest parameters of point clouds generation, was checked using three different software packages (Fig.6).

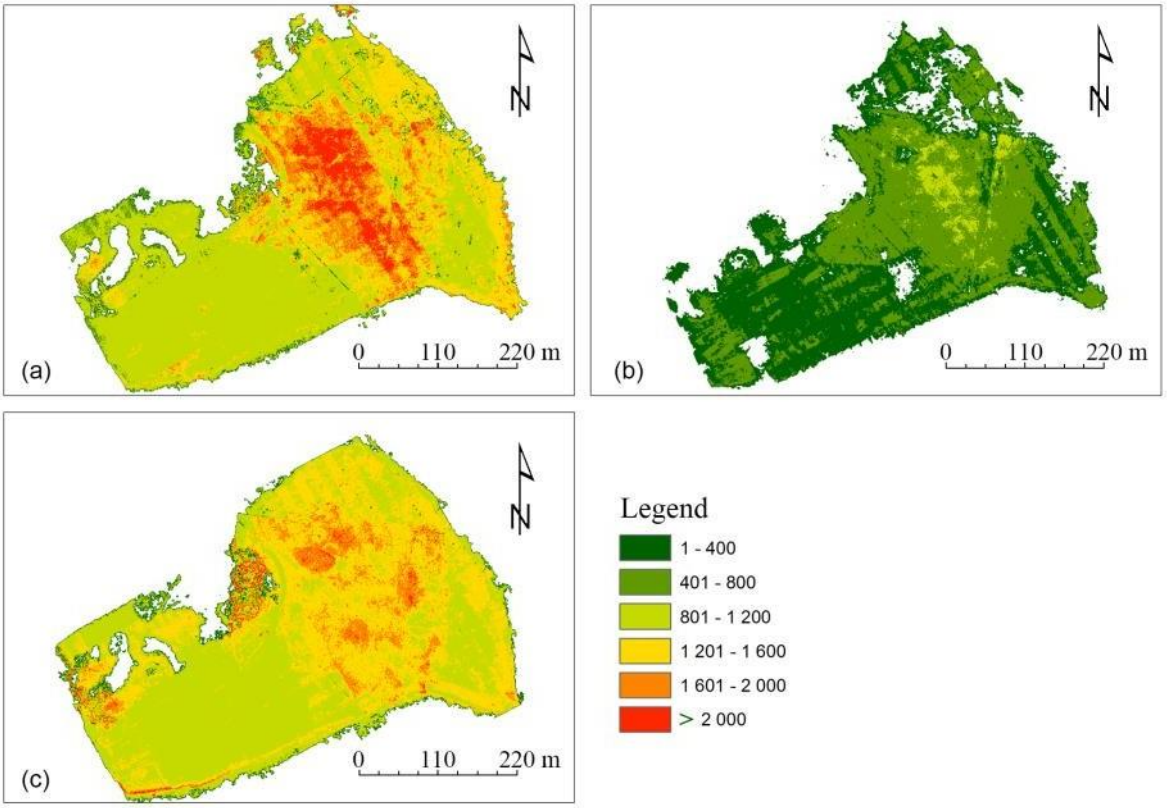

Figure 6. The number of points per 1 sq.m. for the point clouds generated using: a) Pix4D, b) 3D Survey, c) Agisoft Metashape. The colours represent - dark green between 1 and 400, green between 401 and 800, green between 801 and 1200, yellow between 1201 and 1600, orange between 1601 and 2000, red above 2000 points per 1 sq.m

It turns out from Fig.4 that the highest number of points was achieved for the clouds generated using Pix4D, Agisoft Metashape and 3D Survey, respectively. The considerably

DOI:10.55627/smla.001.01.0009

lower number of points per 1 sq.m., detected by the algorithms implemented in Pix4D/Agisoft compared to 3D Survey, may also be noticed.

The distribution of the number of points per 1 sq.m. depending on the fragment of the investigated area was also analysed. For open areas located within the w part of the object, the close values of the number of points per 1 sq.m. may be noted for the point clouds acquired from Pix4D and Agisoft Metashape. In the case of the use of data acquired from the 3D Survey, the number of points varies within the entire area (this may be noticed as diversified shades of the green colour); moreover, blind spots occur in places where points were easily determined by the remaining two software packages. In the case of the central part, where three rows were overlapping and which was covered by low vegetation, it turns out from the number of points per 1 sq.m. that the MVS algorithms implemented in three packages detect the highest number of points (Fig. 6). In the case of re-cultivated areas (the E par), covered by low vegetation and low trees, the highest numbers of points per 1 sq.m. were obtained for the point clouds generated with the use of Pix4D, Agisoft, respectively; a much lower number of points were obtained with the use of data from the 3D Survey package.

Table 6. Statistical characteristics of the number of points per 1 sq.m

Software	Mean	Max	Min
Pix4D	1208	7679	1
3D Survey	430	1319	1
Agisoft Metashape	1223	7717	1

It turns out from the analysis of Table 6 that - on average - the highest number of points per 1 sq.m. was generated using Agisoft Metashape, Pix4D and 3D Survey, respectively. However, it should be noted that in the case of the mean value, the difference between the number of points per 1 sq.m. generated with the use of the 3D Survey is approximately four times smaller compared to other packages; in the case of the maximum value, it is even seven times smaller. Comparing the results obtained for the point clouds generated with Pix4D and Agisoft, it may be noted that both the mean and the maximum numbers of points are similar.

In order to analyse the possibilities of using particular software packages for the inventory of mines and post-mining objects, the number of points per 1 sq.m. was tested on the ground. It was necessary to perform the filtration of the raw point cloud to distinguish points that corresponded only to the ground. Algorithms embedded in particular algorithms were applied. In Pix4D, there is no filtration of points to the ground; the DTM may be generated. The algorithm uses the generated DSM to create the DTM. There is no need to conduct the point cloud classification. Masks of elements, which do not correspond to the ground, are determined. As a result, Pix4D exports the DTM in the GRID (raster) format. The minimum DTM grid size has to be five times bigger than the grid size of the acquired images. For the remaining algorithms, newly generated point clouds are recorded in the LAS format. Table 7 presents the statistical data related to those issues [45].

Table 7. Statistical characteristics of the number of points after filtration to the ground

Software	Number of points	Never classified [%]	Ground [%]	Noise [%]
Pix4D	no data	no data	no data	no data
3D Survey	59 018 158	79.9	20.1	no data
Agisoft Metashape	223 838 028	59.7	39.7	0.6

DOI:10.55627/smla.001.01.0009

It turns out from Table 7 that each implemented algorithm is filtering a completely different number of points to the class “ground”. This is caused by the number of all generated points. That is also why it is necessary to test the distribution of the number of points per 1 sq.m. (Fig. 7).

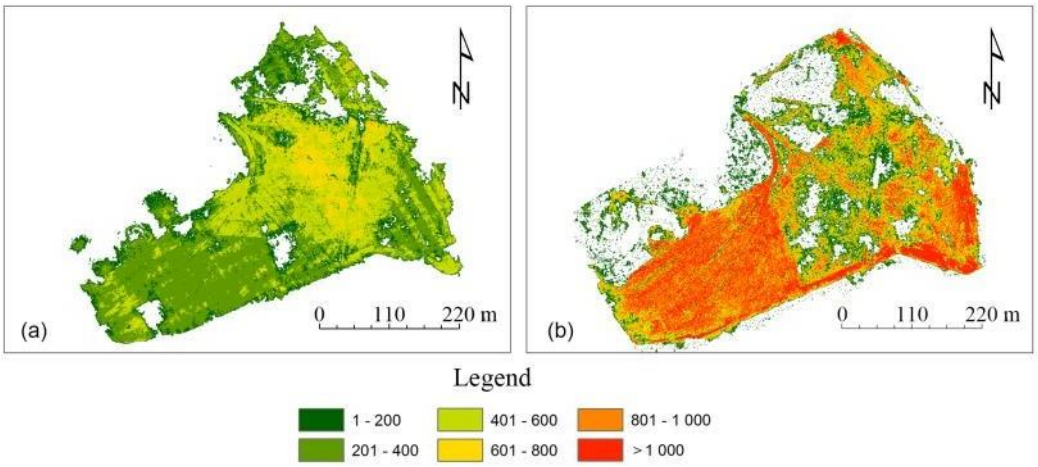

Figure 7. The number of points per 1 sq.m. for point clouds after filtration to the ground: a) 3D Survey, b) Agisoft Metashape

Table 8. Statistical characteristics of the number of points per 1 sq.m. after filtration to the ground

Software	Mean	Max	Min
Pix4D	no data	no data	no data
3D Survey	355	1002	1
Agisoft Metashape	653	1566	1

It turns out from the analysis in Table 8 that - as the average - the highest number of points per 1 sq.m. was generated using Agisoft Metashape and 3D Survey. However, it should be noted that in the case of the mean value, the difference between the number of points per 1 sq.m. of the cloud generated with the 3D Survey is approximately two times smaller.

In order to perform the independent control, the clouds generated with the Pix4D, Agisoft and 3D Survey packages were compared with the results of the geodetic surveys. In this step, 1542 GNSS and RTK points were used, which were not utilised in the bundle adjustment process. Among others, the following results were analysed:

- RMSE values, the maximum and the minimum differences of elevations between DTMs generated in ArcGIS (GRID size 0.1 m) and spot heights (Tab. 9),
- The percentage of points for which the error values are greater than 0.2 mm (Tab. 8),
- Histograms of the elevation error values (Fig. 8) between DTMs and spot heights.

Table 9 presents the statistical data concerning deviations between the points from the GNSS measurements and the DTM generated from Pix4D, Agisoft Metashape and 3D Survey.

DOI:10.55627/smla.001.01.0009

Table 9. Statistical characteristics of the values of the deviations between the points from the GNSS measurements and the DTM (generated in ArcGIS with GRID size 0.1m) developed using particular software applications

Software	Points before filtration			Points after filtration			No. of % for, |v|>0.2 m
	RMSE [m]	v max [m]	v min [m]	RMSE [m]	v max [m]	v min [m]	
Pix4D	0.35	2.26	0.00	0.09	0.20	0.00	33.0
3D Survey	0.99	4.67	0.00	0.11	0.20	0.00	67.6
Agisoft Metashape	0.67	3.77	0.00	0.09	0.20	0.00	53.9

Using the point clouds filtered by different software packages, the Digital Terrain Models were generated in the form of a regular GRID with a 10 cm resolution. For the point clouds acquired from Agisoft Metashape and 3D Survey, ArcGIS was applied, and the point cloud was converted into the DSM using the Pix4D package.

To analyse the obtained results, it was decided to determine the RMSE values, the maximum and the minimum values of the absolute deviations for all spot heights. Following the Polish regulations, in the case of height measurements, the maximum error of measurements, 20 cm, is assumed. Therefore, it was decided to perform filtration of the obtained results, considering points for which the error values were higher than 20 cm.

When the results before filtration are analysed (Tab. 9), it may be noticed that the smaller RMSE value was obtained for the DTM generated from the point cloud acquired in Pix4D - 35 cm, and the highest error value (about 1 metre) was obtained using the 3D Survey package. In the case of absolute maximum values, the worst results were obtained for the DTM generated based on the point cloud from 3D Survey (4.67 m), Agisoft Metashape (3.77m) and Pix4D (2.26m), respectively.

As a result of filtration, the RMSE values for the differences between the DTM generated from point clouds from particular packages and geodetic surveys are similar. They are equal to 11 cm, approximately. As it turns out from the results presented in Table 9, the smallest number of incorrect points were obtained for the DTM generated in Pix4D (about 33%), and the worst results were obtained using the 3D Survey package (about 68%).

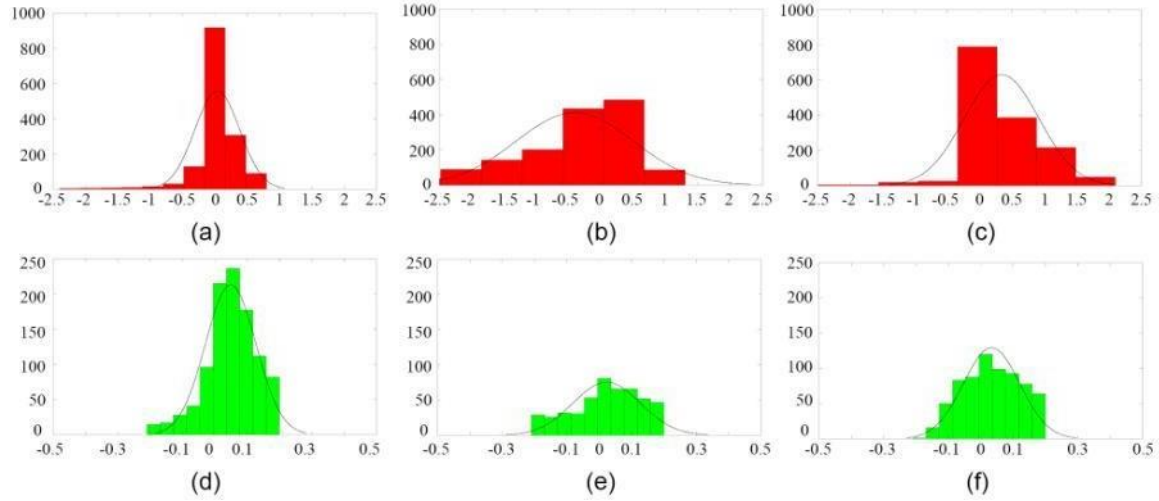

Figure 8. Histograms of the values of the elevation deviations between the points from the GNSS measurements and the DTM acquired from: a) Pix4D - before filtration, b) Pix4D - after filtration, c) 3D Survey - before filtration, d) 3DSurvey - after filtration, e) Agisoft Metashape - before filtration, f) Agisoft Metashape - after filtration

DOI:10.55627/smla.001.01.0009

The histograms in Figure 8 present the distribution of error values for points before filtration (in red) and after filtration - points of the values of deviations greater than 20 cm (in green). Moreover, normal Gauss distribution curves were overlaid on the histograms. It turns out from the analysis of the obtained results that for differences in elevations between the DTM from the photogrammetric data and geodetic surveys, the distribution closest to the normal Gauss distribution is obtained for algorithms implemented in Pix4D (Fig. 8a) and Agisoft Metashape (Fig 8e). The worst results were obtained for 3D Survey. The distribution of errors is not symmetric and is slightly shifted to the right; this proves the presence of systematic errors. In the case of filtered points, the shape closest to the Gauss distribution is obtained for the DTM obtained using Pix4D (Fig. 8b). Similarly, as for the differences in points before filtration, the histogram 8d (3D Survey) presents the impact of systematic errors (the lack of symmetry in relation to 0). In the case of histogram 8f (Agisoft), the Gauss distribution of points is not obtained.

Assuming that Pix4D is the reference software package, the results of particular packages not only point to quantitative or qualitative differences. This only confirms the use of different image processing algorithms. It turns out from the analysis of Table 10 that the RMSE of the differences of the DTM for Agisoft is almost two times smaller than for 3D Survey. However, it should be noted that the absolute value of deviations for Agisoft reaches 16 m, and it is almost three times bigger than in the case of the 3D Survey. It is worth noting that, after filtering points to the ground (the DTM), the RMSE values for Agisoft were reduced to 8 cm, and in the case of the 3D Survey, they were not improved. On the other hand, the absolute value of the maximum error for the Agisoft package was reduced by three times.

5. Discussion

The presented results of the processing of low-cost UAV data in different commercial software applications show the quality of the final documentation based on different factors. The chosen tested area is the sand post-mining pit, which is a flat area with a small height difference SE part, which is typical in Poland. Because the tested area is a partially re-cultivated sand post-mining pit, the tested area was characterised by a low quality repetitive texture. In the performed excrement, the low-cost camera DJI Phantom 3 professional, which has been widely used for surveying projects, was used. The UAV is equipped with a nonmetric low-cost RGB Sony EXMOR camera with a focal length of 3.61 mm and a sensor size of 4.72 x 6.3 mm. One of the main disadvantages of this sensor is the issue with the rolling shutter effect. This problem might be overcome in three different ways. First, it is possible to do so by using the implemented function (adding to the equation the additional coefficients), which is possible in the Pix4D software.

From the analysis of the time required for the orientation of photographs, it may be seen that both processes were performed within two times shorter time frames using Pix4D and 3D Survey than in the case of Agisoft Metashape (Tab. 2). In the case of the dense point cloud generation, the shortest computational time achieved Pix4D, than Agisoft Metashape and the longest in the 3D survey. It should be noted that differences between time processing in Agisoft /Pix4D and 3D survey are almost two times longer.

When the results of the image orientation are analysed, it should be stated that the algorithms implemented in all of the tested applications are based on the SfM approach - BLOB algorithms. In all utilised software packages (Pix4D, Agisoft Metashape and 3D Survey), a similar percentage of oriented photographs was obtained, and not oriented photographs represented the area covered by high vegetation (Tab. 3 and Figs. 4 and 5). Comparing the values of the reprojection error (Tab. 4), it might be noticed that the value of this factor for Pix4D is five times smaller than the value obtained in the 3D Survey and Agisoft

DOI:10.55627/smla.001.01.0009

Metashape software applications. On the other hand, the differences in the maximal values of this error in Agisoft are more than 10 times higher than those achieved in the 3D survey (Tab. 3). For this reason, the impact of self-calibration errors and the rolling shutter on the correctness of the point mapping should be considered. Depending on the software, different distortion parameters were chosen in the self-calibration process. In Pix4D, the following parameters were utilised: focal length (fx and fy), centre coordinates (cx and cy), the radial distortion coefficients k1, k2, k3 and the tangential distortion coefficients p1 and p2 and additional coefficients which compensate for the rolling shutter effect. 3D Survey algorithms were based on the typical distortion parameters (i.e., fx and fy, cx, cy, k1,k2,k3, p1, and p2). However, it did not allow selecting its initial parameters and values, which might be precalibrated. On the other hand, in Agisoft, two groups of parameters could be determined for self-calibration: a) fx and fy, cx, cy, k1,k2,k3, p1 and p2 (similar as in Pix4D and 3D Survey) and b) fx and fy, cx, cy, k1,k2,k3, p1, p2, and skew [43]. These additional parameters did not significantly influence the exterior orientation accuracy but allowed to achieve a symmetric distribution of distortion (Fig. 9).

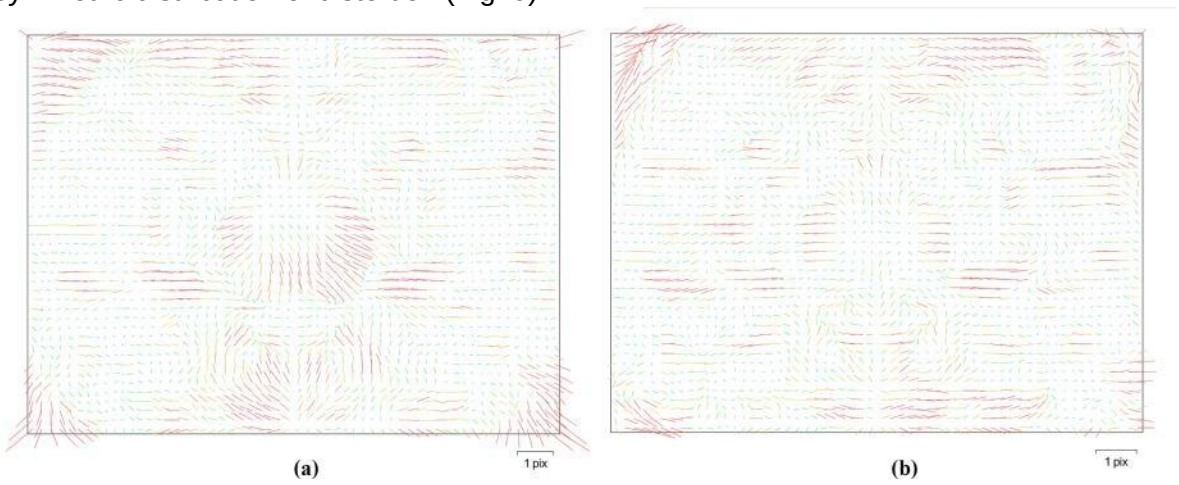

Figure 9. The distribution of image residuals (distortions) based on (a)fx,fy, cx, cy, k1,k2,k3, p1, and p2, (b) fx,fy, cx, cy, k1,k2,k3, p1,p2, and skew coefficient.

For analysing the rolling shutter effect, the accuracy of bundle adjustment (with and without reduction of this error) on control and check points was checked (Tab. 10)

Table 10. Accuracy analysis of the data orientation process on the ground control (11) and check (6) points in Pix4D with and without reducing the rolling shutter effect.

Pix4D	Ground control points			Check points		
	RMSE			RMSE		
	X [m]	Y [m]	Z [m]	X [m]	Y [m]	Z [m]
Not reducing the rolling shutter	0.079	0.107	0.052	0.126	0.200	0.105
Reducing the rolling shutter effect	0.004	0.004	0.019	0.040	0.012	0.063

The results related to the RMSE error before and after the reduction of the rolling shutter effect in the Pix4D software (see Table 10) proved its significant impact on the calibration process.

In order to analyse its influence and accuracy of self-calibration, the authors decided to use the SIFT algorithm to find the corresponding points between the 200 references (Pix4D) and undistorted images from the Agisoft and 3D Survey software applications. For this

DOI:10.55627/smla.001.01.0009

purpose, images from the whole area with different land cover and texture quality were chosen. The results are presented in Table 11.

Table 11. Statistical analysis of points deviation detected with the SIFT algorithm on undistorted images from the Pix4D and Agisoft/3D Survey.

Software	No. points	Deviation					
		Maximum		Minimum		Average	
		u [px]	v [px]	u [px]	v [px]	u [px]	v [px]
Pix4D-3D Survey	7359	2.21	2.89	0.00	0.00	0.49	0.67
Pix4D - Agisoft	7602	5.47	5.43	0.00	0.00	1.67	0.78
Percentage of points deviations							
Software		**> 2 pixels**		**> 3 pixels**		**> 4 pixels**	
		u [%]	**v [%]**	**u [%]**	**v [%]**	**u [%]**	**v [%]**
Pix4D-3D Survey		0.79	0.20	0.04	0.00	0.01	0.00
Pix4D-3D Agisoft		44.93	0.22	19.08	0.02	1.43	0.00

It may be inferred from the analysis of Table 11 that the average deviations between Pix4D and Agisoft for u axis are 3 times higher than between Pix4D and 3D Survey but similar in the case of the v axis. Moreover, the percentage number of points, the deviations of which are higher than 2 pixels for the 3D Survey, is less than 1%. Comparing the different results obtained from Agisoft, it might be noticed that about 45% of points are characterised by deviations higher than 2 pixels, 19% higher than 3 pixels, and about 1.5% higher than 4 pixels.3D Survey can be described as a “black box” dedicated to low-cost UAV data processing (mainly from the excavation areas and sand post-mining sites). Authors believe that in this case, compared to the Agisoft software, it can reduce the rolling shutter effect more efficiently and correctly estimate the distortion parameters in the self-calibration process on poor quality flat areas.

In the process of observation adjustment, key importance is ascribed to the impact of the measurement accuracy, represented in the form of appropriate weighting factors. Such a feature was provided only by Pix4D and the Agisoft Metashape software. The values of the RMSE on control points (Tab. 5) indicate that the lowest accuracy was obtained, respectively, with the use of Agisoft Metashape, 3D Survey and Pix4D. The check point accuracy analysis shows that the height coordinate errors were the biggest ones. It is assumed to reference of the height system differed (the ellipsoid – the geoid). Correct results were obtained only using Pix4D. It should be noted that the correct, approximate reference height influences the value of the Z component of the projection centres obtained directly from georeferencing.

It appeared that the most probable cause of the lower quality results obtained from the 3D Survey (on check points) is due to the exterior orientation algorithm errors. The other important factors, i.e. RMSE reprojection error and elimination of rolling shutter and distortion, were characterised by a satisfactory level of accuracy and did not have that strong negative impact. The article [22] analysed similar problems with low-cost UAV usage in mining areas. In this particular case, DJI Phantom 3 Pro was used. This approach differed only in height deviation over the scanned area and the drone flying height, which was two times higher than in the author’s project. In the case of the image orientation in Agisoft, the control and check points were selected in a similar manner (i.e. number of points and their distribution) as well as initial interior orientation parameters. However, it has to be noted that the accuracy obtained during this project was ten times lower. Differences are mainly caused if the low terrain height deviations are considered. They have a significant negative influence on the self-calibration step. To summarise, the accuracy of all available software applications

DOI:10.55627/smla.001.01.0009

fulfils Polish height measurements regulations where the maximum error allowance is 20 cm.

The obtained results proved that processing the shape of mining and post-mining areas depends on the dense image matching algorithms. Hence, selecting particular algorithms (utilised software packages) is essential. Comparing the results for the products acquired from the 3D Survey (Fig. 10b), a lower accuracy than in the case of Pix4D (Semi-global matching) may be noticed. The best results are obtained for the open area of the W part of the analysed object (green circles, deviation values smaller than 20 cm). In the central part (the re-cultivated fragment, covered by low vegetation) and in the northern part (the re-cultivated fragment, covered by low and high vegetation), the values of the deviations do not exceed 50 cm (yellow circles).

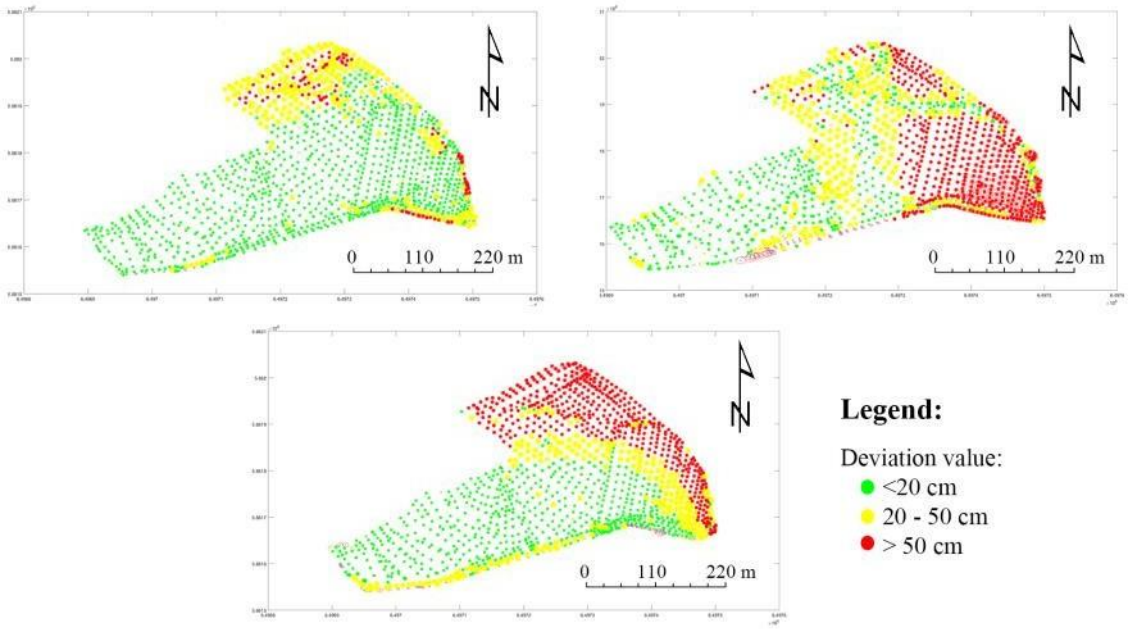

Figure 10. The distribution map of the elevation differences between the points from the GNSS measurements and the DTM was acquired from: a) Pix4D, b) 3D Survey, c) Agisoft Metashape. Points for which the deviation value is less than 20 cm are marked in green; yellow represents deviations larger or equal to 20 cm and less than 50 cm; deviations larger than 50 cm are marked in red. Circles mark the error values rescaled twenty times (in green), fifteen times (yellow) and two times (red)

The worst results were obtained for the south-eastern part of the object (the re-cultivated fragment covered by high and medium vegetation, the area of big differences in height) and on the external fragments of the escarpments. The deviations on points are greater than 50 cm. The obtained results prove incorrect operations of the algorithms for generating dense point clouds and the filtration of point clouds to the points representing the ground.

In the case of the data acquired from Agisoft (depth map fusion algorithms) (Fig. 10c), better results were obtained than in the case of 3D Survey; however, these results were worse than the results obtained from Pix4D. Similarly, as in the case of Pix4D, the smallest height differences between the control points measured using the RTK technique and the DTM were obtained for the western (an open area) and the central part of the analysed object (the re-cultivated fragment, covered by low vegetation).

The worst results were obtained for the northern fragment of the object, where small height differences occur and are covered by low and high vegetation. Compared to the

DOI:10.55627/smla.001.01.0009

results obtained using 3D Survey, considerably better results for the filtered point cloud to the ground points were obtained in the south-eastern part of the analysed area. Differences exceeding 50 cm at the edges of the analysed areas on escarpments may also be noticed.

6. Conclusions

The objective of this paper was to analyse the possibility of the three selected commercial software applications - Pix4D, Agisoft and 3D Survey to process low-cost UAV data acquired for an excavation area and for the sand post-mining site, which, in Poland, are particularly characterised by low height deviations and partly weedy. Unfortunately, in many cases, these areas are used for illegal explorations. Monitoring by low-cost UAV is implemented for the rapid detection of illegal mining and, at the same time, allows to generate the photogrammetric documentation and evaluate the volume of the stolen sand. This information is very helpful for the Polish Geological Institute because this will not only reimburse financial fees but also allow control of the degradation of the landscape.

The paper presents the measurements of an open mine, which were performed using two techniques. Field RTK/GNSS measurements were performed, and RGB photographs were acquired by means of a low-cost UAV platform (DJI Phantom 3 Pro). Three different software packages processed the images: Pix4D, Agisoft Metashape and 3D Survey, which utilise different image processing algorithms, i.e. orientation (SfM) and generation of a dense point cloud (MVS).

In summary, it may be stated that the performed experiments and analyses justified the possibility of using low-cost UAV platforms to monitor mines and post-mining objects. The achieved accuracy of the generated photogrammetric products is comparable with the accuracy of the geodetic surveys. However, the final accuracy depends on the applied software packages, particularly the implemented algorithms.

3D Survey is a software solution for land surveying data processing and is dedicated to mining measurements. Unfortunately, compared to the Pix4D and Agisoft Metashape software applications, the algorithms implemented in 3D Survey do not make it possible to change the initial parameters for camera calibration in the self-calibration process or choosing the weights in bundle adjustment. On the other hand, this application was designed for users who should not have experience in photogrammetry.

To summarise, it might be noticed that choosing the appropriate software depends on different factors, but the most important one is the required accuracy.

In the authors' opinion, this article might be helpful for specialists who work with UAVs (particularly with low-cost UAVs) because of its potential and limitation of using Pix4D, Agisoft Metashape and 3D Survey software in the post-mining flat area or a small height deviations area.

Author Contributions: JM performed the measurements of the photogrammetric network and developed Matlab applications to analyse the results; he also contributed to the analysis of the results. SŁ performed surveys, cooperated in the analysis of the results and is the co-author of the "Introduction" and "Methodology" sections. MP cooperated in writing the "Introduction", "Methodology", and "Discussion" sections. DZ proposed the first draft of the paper, pre-reviewed the entire text and consulted the results of the analyses. VL performed measurements of the photogrammetric control and processed data in 3D Survey, Agisoft and Pix4D. All Authors have read and agreed to the published version of the manuscript.

Funding: This research received no external funding.

Acknowledgements: This research was performed within statutory activities, implemented at the Faculty of Geodesy and Cartography (Warsaw University of Technology) in cooperation with the Polish Geological Institute (National Research Institute), the Faculty of Geology (University of Warsaw) and the Zhytomyr State Technological University.

Authors would like to thank Konrad Górski, Michał Grzyb and Mariusz Pasik for support in the field measurements and Paweł Bylina, Barbara Turbiak and Paweł Karnkowski for providing access to perform measurements in the quartz sand mine in Trzciniec

Conflicts of Interest: The authors declare no conflicts of interest.

References

1. Decree of the Minister of Economy of April 8, 2013 on detailed requirements concerning activity of an open-mining plant (Dz.U. 2013 poz. 1008).
2. Gawin, A. Inventory of a mining excavations of an open brown coal mine using photogrammetric methods. The doctor's thesis, 2015.
3. Pielok, J. Gawałkiewicz, R., Jaśkowski, W., Jura, J., Lipecki, T., Skulich, M., Szafarczyk, A., Szewczyk, J. Mining Geodesy 2011, Publishing in AGH
4. Poręba, M. Modern methods of earth mass volume determination. Archives of Photogrammetry, Cartography and Remote Sensing 2009, 19, 351–361.
5. Zhou, D., Wu, K., Chen, R. et al. GPS/terrestrial 3D laser scanner combined monitoring technology for coal mining subsidence: a case study of a coal mining area in Hebei, China. Nat Hazards 2014, 70: 1197-1208. https://doi.org/10.1007/s11069-013-0868-7.
6. Markiewicz, J. S. and Zawieska, D. Terrestrial scanning or digital images in inventory of monumental objects? – case study, Int. Arch. Photogramm. Remote Sens. Spatial Inf. Sci. 2014, XL-5, 395-400, https://doi.org/10.5194/isprsarchives-XL-5-395-2014.
7. Hu H., Fernandez-Steeger T. M., Dong M., Azzam R. Numerical modelling of LiDAR-based geological model for landslide analysis. Automation in Construction 2012, 24, 184-193.
8. Lipecki, T. Laser scanning in measurements of geometry and deformations of mining objects and installations. Przegląd Górniczy 2010, 66 (7-8), 25-31.
9. Wajs, J. Research on surveying technology applied for DTM modelling and volume computation in open pit mines. Mining Science 2015, 22, 69-77.
10. Patikova, A. Digital photogrammetry in The Practice of Open Pit Mining. In ISPRS XX. Symposium 2004, Commission IV, Wg IV (Vol. 7).
11. Colomina, I., Molina, P. Unmanned aerial systems for photogrammetry and remote sensing: A review. ISPRS Journal of Photogrammetry and Remote Sensing 2014, 92, 79-97. https://doi.org/10.1016/ j.isprsjprs.2014.02.013.
12. Bakuła, K., Ostrowski, W., Szender, M., Plutecki, W., Salach, A., Górski, K. Possibilities for Using LIDAR and Photogrammetric Data Obtained with AN Unmanned Aerial Vehicle for Levee Monitoring. The International Archives of the Photogrammetry, Remote Sensing and Spatial Information Sciences 2016, XLI-B1.
13. Gómez-Candón, D., De Castro, A. I., López-Granados, F. Assessing the accuracy of mosaics from unmanned aerial vehicle (UAV) imagery for precision agriculture purposes in wheat. Precision Agriculture 2014, 15(1), 44-56. https://10.1007/s11119-013-9335-4.
14. Bachmann, F., Herbst, R., Gebbers, R., Hafner, V. V. Micro UAV based georeferenced orthophoto generation in VIS+ NIR for precision agriculture. Int. Arch. Photogramm. Remote Sens. Spat. Inf. Sci 2013, 11-16, doi: 10.5194/isprsarchives-XL-1-W2-11-2013
15. Lee, S., Choi, Y. Reviews of unmanned aerial vehicle (drone) technology trends and its applications in the mining industry. Geosystem Engineering 2016, 19(4), 197-204. https://doi.org/10.1080/ 12269328.2016.1162115.
16. Shahbazi, M., Sohn, G., Théau, J., Ménard, P. UAV-based point cloud generation for open-pit mine modelling. The International Archives of Photogrammetry, Remote Sensing and Spatial

Information Sciences 2015, 40(1), 313. https://doi.org/10.5194/isprsarchives-XL-1-W4-313-2015.
17. Siebert, S., Teizer, J. Mobile 3D mapping for surveying earthwork projects using an Unmanned Aerial Vehicle (UAV) system. Automation in Construction 2014, 41, 1-14. https://doi.org/10.1016/j.autcon.2014.01.004.
18. Smith, M.W., Carrivick, J.L., Quincey, D.J. Structure from motion photogrammetry in physical geography, 2016, Progress in Physical Geography, Vol. 40(2) 247–275
19. Tscharf, A., Rumpler, M., Fraundorfer, F., Mayer, G., Bischof, H. On the use of UAVs in mining and archaeology - geo-accurate 3d reconstructions using various platforms and terrestrial views, ISPRS Ann. Photogramm. Remote Sens. Spatial Inf. Sci. 2015, II-1/W1, 15-22, https://doi.org/10.5194/
isprsannals-II-1-W1-15-2015.
20. Yucel, M. A., Turan, R. Y. Areal change detection and 3D modelling of mine lakes using high-resolution unmanned aerial vehicle images. Arabian Journal for Science and Engineering 2016, 41(12), 4867-4878. https://doi.org/10.1007/s13369-016-2182-7.
21. Vasuki, Y., Holden, P., Kovesi, P., Micklethwaite, S. Semi-automatic mapping of geological Structures using UAV-based photogrammetric data: An image analysis approach. Computers & Geosciences 2014, 69, 22-32. https://doi.org/10.1016/j.cageo.2014.04.012.
22. Tien Bui, D., Long Nguyen, Q., Nam Bui, X., Nghia Nguyen, V., Van Pham, C., Van Le, C., Thao Thi Ngo, P., Tien Bui, D., Kristoffersen, B. Lightweight Unmanned Aerial Vehicle and Structure from Motion Photogrammetry for Generating Digital Surface Model for Open Pit Coal Mine Area and Its Accuracy Assessment. 2017, 10.1007/978-3-319-68240-2_2
23. Vautherin, J., Rutishauser, S., Schneider-Zapp, K., Choi, H. F., Chovancova, V., Glass, A., Strecha, C. Photogrammetric accuracy and modelling of rolling shutter cameras. ISPRS Annals of Photogrammetry, Remote Sensing & Spatial Information Sciences 2016, 3(3).
24. Al-Rawabdeh, A., He, F., Moussa, A., El-Sheimy, N., Habib, A. Using an unmanned aerial vehicle-based digital imaging system to derive a 3D point cloud for landslide scarp recognition. Remote Sensing, 2016, 8(2), 95.
25. Jeong, H. H., Park, J. W., Kim, J. S., and Choi, C. U. Assessing the Accuracy of Ortho-image using Photogrammetric Unmanned Aerial System, Int. Arch. Photogramm. Remote Sens. Spatial Inf. Sci. 2016, XLI-B1, 867-872, https://doi.org/10.5194/isprs-archives-XLI-B1-867-2016, 2016.
26. Jaud, M.; Passot, S.; Le Bivic, R.; Delacourt, C.; Grandjean, P.; Le Dantec, N. Assessing the Accuracy of High Resolution Digital Surface Models Computed by PhotoScan® and MicMac® in Sub-Optimal Survey Conditions. *Remote Sens.* **2016**, *8*, 46
27. Tong, X., Liu, X., Chen, P., Liu, S., Luan, K., Li, L., Hong, Z. Integration of UAV-based photogrammetry and terrestrial laser scanning for the three-dimensional mapping and monitoring of open-pit mine areas. Remote Sensing, 2015, 7(6), 6635-6662.
28. Kovanič, Ľ., Blistan, P., Zelizňaková, V., Palková, J. Surveying of Open Pit Mine Using Low-Cost Aerial Photogrammetry, 2017, In book: The Rise of Big Spatial Data, pp.121-129, DOI: 10.1007/978-3-319-45123-7_9
29. Shahbazi, M., Sohn, G., Théau, J., Menard, P. Development and Evaluation of a UAV-Photogrammetry System for Precise 3D Environmental Modeling. Sensors, 2015, 15. 27493-27524. 10.3390/s151127493.
30. Bednarczyk, Z. Landslide Monitoring and Counteraction Technologies in Polish Lignite Opencast Mines, 2017, In Automatic Landslides Mapping in the Principal Component Domain, pp.33-43.
31. Remondino F., El-Hakim S. Image-Based 3d Modelling: A Review, (w:) The Photogrametric Record 2006, s. 269–291. MVS.
32. Sona, G.; Pinto, L.; Pagliari, D.; Passoni, D.; Gini, R. Experimental analysis of different software packages for orientation and digital surface modelling from UAV images. Earth Science Informatics 2014, 7(2), 97–107. https://doi.org/10.1007/s12145-013-0142-2.

33. Ai, M., Hu, Q., Li, J., Wang, M., Yuan, H., Wang, S. A robust photogrammetric processing method of low-altitude UAV images. Remote Sens. 2015, 7(3), 2302-2333; doi:10.3390/rs70302302
34. Moussa W. Integration of Digital Photogrammetry and Laser Scanning for Cultural Heritage Data2006 Recording, (w:):http://citeseerx.ist.psu.edu/viewdoc/download?doi=10.1.1.65.6104&rep=rep1&amp.
35. Stylianidis, E., Remondino, F. 3D Recording, Documentation and Management of CulturalHeritage, (w:) Whittles Publishing MVS 2016, ISBN 978-1498763035.
36. Tuytelaars, T. and Mikolajczyk, K. Local invariant feature detectors: a survey. Foundations and Trends in Computer Graphics and Vision 2008, (3), pp. 177–280.
37. Urban, S. and Weinmann, M. Finding A Good Feature Detector -Descriptor combination For The 2d Keypoint -Based Registration Of TLS Point Clouds, ISPRS nn. Photogramm. Remote Sens. Spatial Inf. Sci. 2015, I-3/W5, 121-128, doi:10.5194/isprsannals-I-3-W5-121-2015.
38. Liang, C. K., Chang, L. W., Chen, H. H. Analysis and compensation of rolling shutter effect. IEEE Transactions on Image Processing, 2008, 17(8), 1323-1330.
39. Battiato, S., Curti, S., La Cascia, M., Tortora, M., Scordato, E. Depth map generation by image classification. In Proceedings of SPIE 2004, Vol. 5302, pp. 95-104.
40. Häne, C., Zach, C., Lim, J., Ranganathan, A., Pollefeys, M. Stereo depth map fusion for robot navigation. Intelligent Robots and Systems (IROS) 2011, 2011 IEEE/RSJ International Conference on (pp. 1618-1625).
41. Bhandari, B., Oli, U., Pudasaini, U., Panta, N. Generation of High Resolution DSM Using UAV Images. In FIG Working Week 2015, (pp. 17-21).
42. Hirschmuller, H. Accurate and efficient stereo processing by semi-global matching and mutual information. In Computer Vision and Pattern Recognition 2005. CVPR 2005. IEEE Computer Society Conference on (Vol. 2, pp. 807-814).
43. Hirschmüller, H. Semi-global matching-motivation, developments and applications. Photogrammetric Week 11, 2011, 173-184.
44. Percoco, P., Guerra M., G., Salmeron, J., S., Galantucci, L., M. Experimental investigation on camera calibration for 3D photogrammetric scanning of micro-features for micrometric resolution. The International Journal of Advanced Manufacturing Technology 2017, Vol. 91 (Issue 9-12), 2935 - 2947, DOI: 10.1007/s00170-016-9949-6.
45. Tutorial of Pix4D Video Academy 13 - DTM and Contour Lines (https://www.youtube.com/watch?v=NjCiTHTKXr8&t=126s (Available :08.11.2017))